Further investigations into tetrahedral M_4L_6 cage complexes containing guest anions: new structures and NMR spectroscopic studies†‡

Ian S. Tidmarsh,[a] Brian F. Taylor,[a] Michaele J. Hardie,[b] Luca Russo,[c] William Clegg[c] and Michael D. Ward*[a]

Received (in Montpellier, France) 26th September 2008, Accepted 11th November 2008
First published as an Advance Article on the web 2nd December 2008
DOI: 10.1039/b816864d

A series of ligands L^{Ph}, L^{naph} and L^{anth}, which contain two bidentate pyrazolyl–pyridine termini separated by an aromatic (1,2-phenyl, 2,3-naphthyl or 2,3-anthracenyl, respectively) spacer have been used to prepare tetrahedral cage complexes of the form $[M_4L_6]X_n$, in which a bis-bidentate bridging ligand spans each of the six edges of the M_4 tetrahedron and one anion is bound in the central cavity. Several new examples have been structurally characterised, including an example with a new ligand (L^{anth}), the first example with a second-row transition metal ion [Cd(II)], and the first example of a cage containing a dianionic guest (hexafluorosilicate). The series of structurally similar Co(II) complexes $[Co_4L_6(BF_4)](BF_4)_7$ (L = L^{Ph}, L^{naph} and L^{anth}) have been examined in detail by NMR spectroscopy. The ^{1}H NMR spectra are highly shifted between −110 and +90 ppm, but the spectra can be completely assigned by correlation of measured T_1 relaxation times with distances of the protons in the complexes from the paramagnetic Co(II) centres. ^{1}H DOSY measurements have been used to estimate diffusion constants which confirm the structural integrity of the cages in solution, and ^{19}F DOSY measurements on the anions show that (i) the trapped $[BF_4]^-$ anion diffuses at the same rate as the cage superstructure surrounding it, indicating that it is trapped inside the cage cavity; and (ii) the 'free' $[BF_4]^-$ anions have diffusion rates consistent with substantial retardation due to ion-pairing with the 7+ complex cation.

Introduction

Polyhedral coordination cages have attracted much attention over the last few years[1–9] due to a combination of (i) their elegant and appealing structures, which arise in many cases from very simple combinations of metal ions and bridging ligands,[1,2] and (ii) their host–guest chemistry which allows them in some cases to stabilise otherwise inaccessible species and to behave as 'microreactors'.[3,4] The basic symmetry and stoichiometry principles which underpin their synthesis have been exploited by many groups who have prepared remarkably elaborate cage complexes.

The archetype of this type of complex is the M_4L_6 tetrahedral cage in which four metal ions, forming the vertices of a tetrahedron, are coordinated by six bis-bidentate bridging ligands, each of which spans one of the six edges of the tetrahedron.[5] Each metal ion (at a vertex) is thus coordinated by three bidentate ligand termini (from the three edges which meet at that vertex), and each ligand bridges two metal ions. Four six-coordinate metal ions require 24 donor atoms, which are exactly provided by the six bis-bidentate bridging ligands, and it is significant that the 4 : 6 metal–ligand ratio—which is required for this stoichiometric reason—exactly matches the vertex to edge ratio of the simplest Platonic solid. The first cage of this type was reported by Saalfrank *et al.*,[10] since when many examples have been prepared by other groups.[5] Sometimes, a counter-ion is trapped in the central cavity and it may even act as a template for the cage-assembly process.[5f]

We reported a while ago a series of such tetrahedral cages based on bridging ligands L^{Ph} and L^{naph} (shown in Scheme 1), in which two bidentate pyrazolyl–pyridine chelates are connected by a central aromatic spacer.[5b,f,g] These afford, with Co(II) and Zn(II) as cation and perchlorate or tetrafluoroborate as the anion, cages in which a counter-ion is tightly bound in the central cavity, and in fact the counter-ion templates the cage assembly.[5f] All of the examples that we have isolated have been based on (high-spin) Co(II) or Zn(II) which have similar ionic radii in six-coordinate environments (88 pm in both cases); attempts to prepare analogous Ni(II) cages have never succeeded because the slightly smaller ionic radius (83 pm in octahedral coordination) would make a cage structure too crowded, and instead simpler complexes of the type $[Ni_2L_3]X_4$ were isolated.[5b,f] Also, all examples of M_4L_6 cages with L^{Ph} and L^{naph} have used perchlorate or tetrafluoroborate as the anion;[5b,f,g] these anions are ideal in terms of size and shape for the central cavity of the cages. A notable feature of $[Zn_4(L^{naph})_6(BF_4)](BF_4)_7$ is that the aromatic stacking between ligands around the periphery of the cage, in which the naphthyl groups are involved, results in a red-shifted exciplex-type luminescence from the naphthyl groups which

[a] *Department of Chemistry, University of Sheffield, Sheffield, UK S3 7HF*
[b] *School of Chemistry, University of Leeds, Leeds, UK LS2 9JT*
[c] *School of Chemistry, Newcastle University, Newcastle upon Tyne, UK NE1 7RU*

† Dedicated to Prof. Jean-Pierre Sauvage on the occasion of his 65th birthday.

‡ CCDC reference numbers 708981–708985. For crystallographic data in CIF or other electronic format see DOI: 10.1039/b816864d

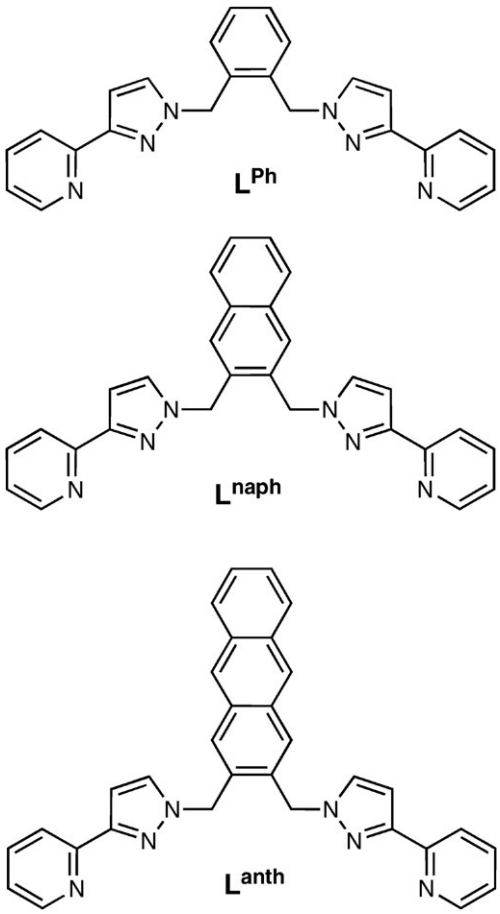

Scheme 1

is diagnostic of the assembled cages since the free ligand L^{naph} shows only normal naphthyl-based luminescence.[11]

In this paper we report a series of further studies on this family of cage complexes. Firstly, we have prepared the new fluorescent ligand L^{anth} (Scheme 1) and studied the structure and photophysical properties of its Zn(II) cage; this follows our previous work with L^{naph} and its Zn(II) cage.[11] Secondly, we describe the structures of some new cage complexes with L^{naph}, with different metals and counter-ions; in particular we describe a cage which contains hexafluorosilicate as the anion, the first example in this series of a dianionic guest, thereby extending the range of encapsulated guest species that are available to this series of cages. Finally, a detailed NMR analysis has been undertaken of the three paramagnetic Co(II) complexes which has allowed full assignment of the highly-shifted spectra based on T_1 measurements; these cages have also been investigated by DOSY NMR spectroscopy to examine their structural integrity in solution.

Results and discussion

(i) Synthesis of L^{anth} and the structure and luminescence properties of its Zn(II) cage complex

Previously we have reported M_4L_6 cage complexes based on the ligands L^{Ph} and L^{naph}.[5b,f,g] To add to this set we have now prepared L^{anth} (Scheme 1) which was prepared by reaction of

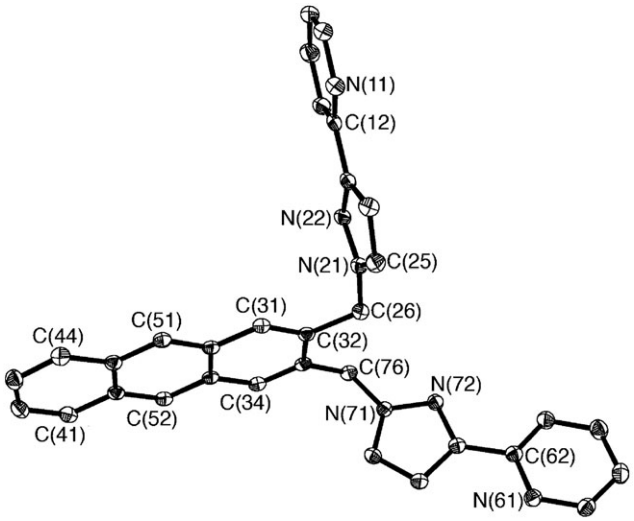

Fig. 1 Molecular structure of L^{anth} showing 40% displacement ellipsoids.

2,3-bis(bromomethyl)anthracene with two equivalents of 3-(2-pyridyl)pyrazole under basic conditions in the usual way, and satisfactorily characterised by ^{1}H NMR spectroscopy and mass spectrometry. The molecular structure of L^{anth} from crystallographic data is shown in Fig. 1 (see Table 1 for all crystallographic data). Bond lengths and angles within the molecule are unremarkable. The two pyrazoyl rings containing N(21) and N(71) are both oriented such that they are near-perpendicular to the central anthracenyl unit, with angles between pyrazolyl/anthracenyl mean planes of 86° and 84°, respectively. In addition the two pyrazolyl rings are almost orthogonal to one another (83°), such that those three π-systems (pyrazolyl/anthracenyl/pyrazolyl) are essentially mutually perpendicular, which facilitates extensive intermolecular interactions involving the aromatic rings. These interactions are dominated by CH···π stacking between C(25)–H(25) of a pyrazolyl ring in one molecules and the anthracenyl unit in another [distance between H(25) and mean plane of anthracenyl system, 2.59 Å], and offset face-to-face stacking of a parallel pair of anthracenyl units (average separation between mean planes, 3.35 Å), and also face-to-face stacking of pyrazolyl rings [N(71)–C(75)] between an adjacent pair of molecules (average separation between mean planes, 3.29 Å).

Reaction of L^{anth} with $Zn(BF_4)_2$ in the required 3 : 2 ratio in MeOH under solvothermal conditions followed by slow cooling afforded a crop of crystals of $[Zn_4(L^{anth})_6(BF_4)](BF_4)_7$. An X-ray crystallographic study was attempted and was partially successful. The crystals, even though of a good size and well-formed, scattered very weakly due to severe disorder in which both enantiomers of the cage overlap with one another, such that many atoms had a site occupancy of 0.5, but when two atoms from the two disordered components occupied the same site the site could be refined with a site occupancy of 1.0. All metal atoms were disordered over two sites. Solvent molecules and counter-ions also exhibited disorder. As a consequence, even when using X-rays from a rotating anode source, the conventional *R*-factor was about

Table 1 Crystallographic data for the new compounds

Compound	L^{anth}	$[Zn_4(L^{anth})_6(BF_4)](BF_4)_7$	$[Cd_4(L^{naph})_6(BF_4)](BF_4)_7 \cdot 5MeOH \cdot 3H_2O$	$[Cd(L^{naph})(BF_4)](BF_4) \cdot 2MeNO_2$	$[Zn_4(L^{naph})_6(SiF_6)](SiF_6)_3$
Formula	$C_{32}H_{24}N_6$	$C_{192}H_{144}B_8F_{32}N_{36}Zn_4$	$C_{173}H_{158}B_8Cd_4F_{32}N_{36}O_8$	$C_{30}H_{28}B_2CdF_8N_8O_4$	$C_{168}H_{132}F_{24}N_{36}Si_4Zn_4$
Molecular weight	492.57	3911.39	4013.43	850.62	3484.94
Habit	Yellow prism	Colourless block	Colourless block	Colourless plate	Colourless block
T/K	150(2)	150(2)	150(2)	150(2)	120(2)
Crystal system	Triclinic	Rhombohedral	Monoclinic	Monoclinic	Cubic
Space group	P-1	R-3	$P2_1/c$	$P2_1/c$	Pa-3
a/Å	9.7446(9)	19.8865(6)	22.0402(7)	16.0291(3)	32.973(10)
b/Å	11.5028(11)	19.8865(6)	19.5943(6)	13.6181(3)	32.973(10)
c/Å	11.7836(11)	48.236(3)	43.0372(13)	16.6842(3)	32.973(10)
α/°	98.106(6)	90	90	90	90
β/°	98.719(6)	90	92.863(2)	117.256(1)	90
γ/°	100.454(6)	120	90	90	90
V/Å^3	1264.5(2)	16520.2(13)	18562.9(10)	3237.56(11)	35849(19)
Z	2	3	4	4	8
ρ/g cm^{-3}	1.294	1.179	1.436	1.745	1.291
Crystal size/mm^3	0.30 × 0.25 × 0.10	0.14 × 0.12 × 0.05	0.80 × 0.40 × 0.20	0.60 × 0.40 × 0.40	0.14 × 0.12 × 0.05
μ/mm^{-1}	0.079	0.511	0.549	0.773	0.639
Data, restraints, parameters	5148, 0, 343	4820, 178, 268	31653, 228, 2217	7425, 0, 480	8337, 117, 247
Final R, R_w[a]	0.0394, 0.1041	0.1872, 0.5105	0.1148, 0.2849	0.0381, 0.0943	0.1578, 0.4761

[a] The value of R is based on 'observed' data with $I > 2\sigma(I)$; the value of R_w is based on F^2 values all data.

0.19. Accordingly we will not discuss the structure in any detail but just note that the basic connectivity and gross structure of the cage are the same as in other members of this series (Fig. 2). Each complex cation is chiral with all four tris-chelate metal centres having the same chirality, affording (non-crystallographic) T symmetry; the central cavity contains a tetrafluoroborate anion which is inverted with respect to the M_4 tetrahedron; and the anthracenyl group of each ligand is sandwiched between coordinated pyridyl–pyrazolyl units from two adjacent ligands. The aromatic rings of the anthracenyl units do not completely overlap with the pyridyl–pyrazolyl rings on either side, but the offset between them will result in interactions in which pyridyl H^3 and pyrazolyl H^4 protons lie above and below the anthracene π-cloud; and anthracenyl protons H^1, H^4, H^9 and H^{10} will lie above the π-clouds of coordinated pyridyl rings [Fig. 2(b)]. The Zn···Zn separations along the edges of the tetrahedron are all *ca.* 9.7 Å.

$[Zn_4(L^{anth})_6(BF_4)](BF_4)_7$ was further characterised on the basis of its ^{1}H NMR spectrum (Fig. 3) which also shows the spectrum of free L^{anth}. The spectrum shows 12 independent proton environments, indicating that all ligands are equivalent and all have two-fold symmetry, such that only half of one ligand is in a magnetically unique environment with the others being symmetry related. This is consistent with the presence of T symmetry which will generate four C_3 axes, one through each metal vertex, as well as three mutually perpendicular C_2 axes passing through the edges of the tetrahedron. It is noticeable that several of the resonances of the free ligand have moved substantially to lower chemical shift positions in the complex, in part due to aromatic π-stacking between ligands which results in protons being shielded by ring-current effects. The singlet due to anthryl protons H^1/H^4 has shifted from 7.8 ppm in the free ligand to 6.0 in the complex for this reason, and other shifts are marked in Fig. 3. Note also that the singlet at 5.6 ppm for the CH_2 protons of the free ligand has become an AB multiplet (5.3 ppm) in the complex because, in the chiral cage, the two protons are diastereotopic and hence couple to one another. In addition, the ^{19}F NMR spectrum of $[Zn_4(L^{anth})_6(BF_4)](BF_4)_7$ shows two signals in a 7 : 1 ratio, corresponding to the external (free, −151 ppm) and internal (trapped, −140 ppm) anions, respectively, providing additional evidence that the cage retains its structural integrity in solution.

We were interested to see the extent to which the fluorescence of the anthracene unit in L^{anth} was modified by being stacked with other ligands in the assembled cage. Accordingly we compared the fluorescence spectra of free L^{anth} and $[Zn_4(L^{anth})_6(BF_4)](BF_4)_7$ in MeCN. The two spectra are almost identical, showing an unremarkable and typical anthracene-based fluorescence profile whose highest-energy component is at 390 nm, with no evidence of a lower-energy emission band from the cage. This contrasts with the behaviour of L^{naph11} and other naphthyl-based ligands[12] which are stacked in cage assemblies, implying that the fluorescent excited state in L^{anth} is not significantly perturbed by the stacking interactions in adjacent ligands. This seems surprising in view of the structural similarity between the cages with L^{naph} and L^{anth}, and we speculate that it may be due to the larger size of the anthryl group which results in a smaller part of its surface area being involved in π-stacking interactions compared to L^{naph} [*cf.* Fig. 2(b)].

(ii) Structural studies on new cage complexes incorporating different metal ions and counter-ions

As mentioned earlier, all of the structurally characterised cage complexes with this series of ligands have arisen using Co(II) or Zn(II) as the metal ion (which have the same ionic radius in octahedral geometry) and tetrafluoroborate or perchlorate as the tetrahedral guest anion.[5b,f,g] A slightly smaller cation such as Ni(II) gives open-chain dinuclear species $[LNi(\mu\text{-}L)NiL]^{4+}$, with two tetradentate chelating terminal ligands and one

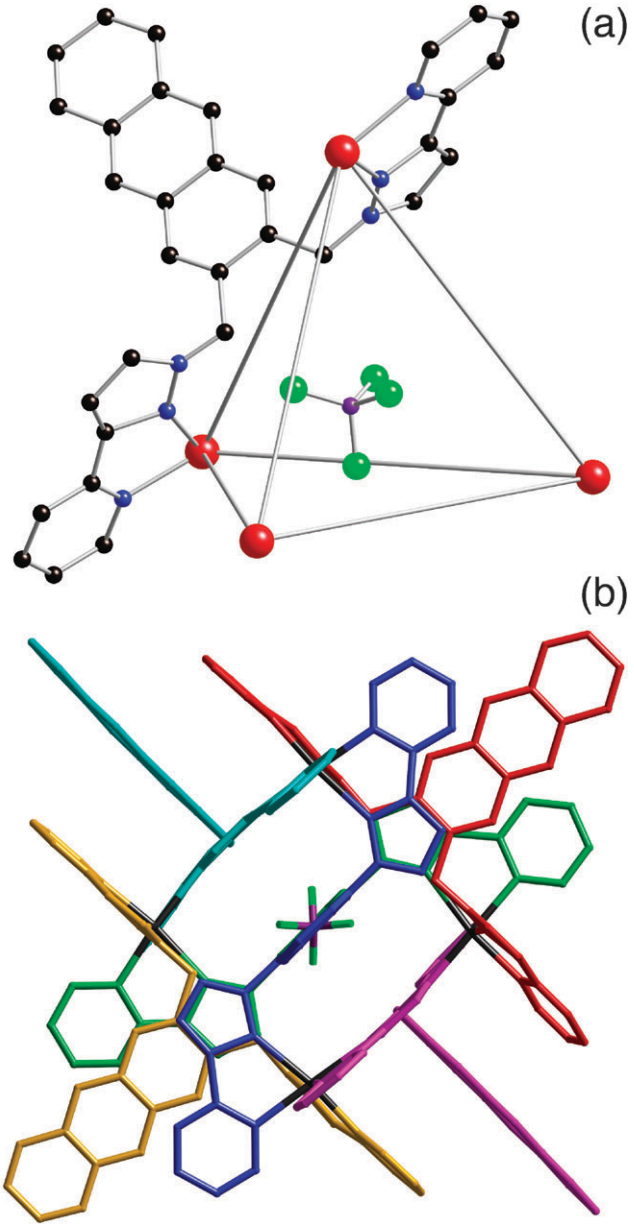

Fig. 2 Two views of the complex cation of $[Zn_4(L^{anth})_6(BF_4)](BF_4)_7$, with only one of the two disordered components shown. (a) A view showing the tetrahedral arrangement of Zn(II) ions, one bridging ligand, and the encapsulated anion: atom colours are black for C, blue for N, red for Zn, purple for B and green for F. (b) A view of the complete complex cage (plus encapsulated anion) with each ligand coloured separately.

bridging ligand,[5b,f] because the shortening of metal–ligand bonds and compression of the coordination sphere cannot be accommodated in a cage structure that is already tightly packed.

We were interested therefore to see if larger cations still resulted in this type of cage structure, so we investigated the reaction of L^{naph} with $Cd(BF_4)_2$ in a 3 : 2 ratio under both ambient conditions (preparation in MeOH–$CHCl_3$ and crystallisation from nitromethane) and solvothermal conditions (using MeOH as solvent, followed by slow cooling). Both types of preparation afforded batches of solid material whose

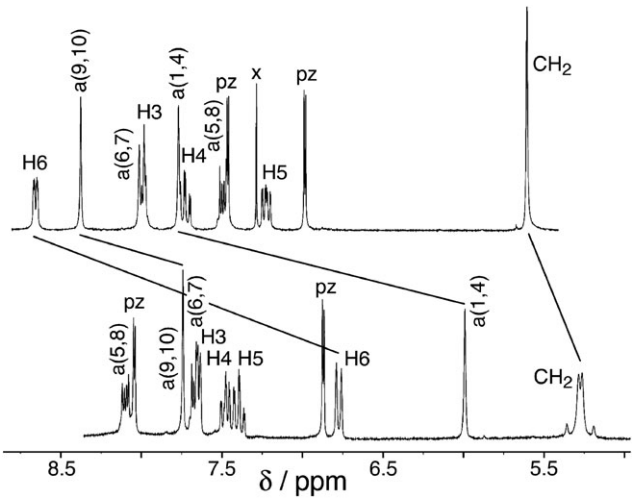

Fig. 3 250 MHz ^1H NMR spectra of (top) L^{anth} in $CDCl_3$ and (bottom) $[Zn_4(L^{anth})_6(BF_4)](BF_4)_7$ in CD_3CN. Assignments were made on the basis of ^1H–^1H COSY spectra. Some signals that have shifted significantly are connected by solid lines between the two spectra. The labels H3, H4 *etc.* denote the protons on the pyridyl rings; pz denotes a proton from the pyrazolyl ring; a(1,4) denotes protons H^1 and H^4 of the anthracenyl group *etc.* The 'x' on the top spectrum denotes the signal for residual protonated $CHCl_3$.

NMR spectrum clearly showed the presence of a mixture of two species in somewhat varying proportions but with obvious major and minor components having signal intensities in a ratio of *ca.* 8 : 1. Both components consisted of a set of signals appropriate for an L^{naph} ligand with two-fold symmetry—*i.e.* one-half of the ligand is unique—but in a chiral environment, with the diastereotopic CH_2 signals appearing as a pair of doublets.

Crystallisation of the crude product from nitromethane–ether afforded crystals of what proved to be two different compounds, although the crystal habits were not obviously different. One set of crystals proved, on analysis, to be the simple 1 : 1 complex $[Cd(L^{naph})(BF_4)](BF_4)$ in which one molecule of L^{naph} coordinates to Cd(II) as a simple tetradentate chelate with the Cd–N distances lying in the range 2.24–2.33 Å (Fig. 4). The five-fold coordination is completed by coordination of an F atom from a $[BF_4]^-$ anion (Cd···F, 2.44 Å); the τ parameter[13] is 0.27, indicating that the structure is closer to a square pyramid ($\tau = 0$) than a trigonal bipyramid ($\tau = 1$). Although this structure is in itself unremarkable, it is interesting that moving from small Co(II)/Zn(II) ions to the larger and 'softer' Cd(II) ion appears to weaken the strong driving force for anion-templated formation of a tetrahedral cage and allow alternative possibilities.

The other crystalline product proved to be the cage $[Cd_4(L^{naph})_6(BF_4)](BF_4)_7$ (Fig. 5). This has the characteristic structure of other cages with this series of ligands, with (non-crystallographic) *T* symmetry, and all metal centres in one cage molecule having the same chirality (the crystal structure as a whole is racemic). Every ligand within a cage is thus twisted in the same sense. The central $[BF_4]^-$ anion is inverted with respect to the Cd_4 tetrahedron, such that each F atom is directed towards the centre of a face of the cage, where it interacts with the protons of the three CH_2 groups that lie in

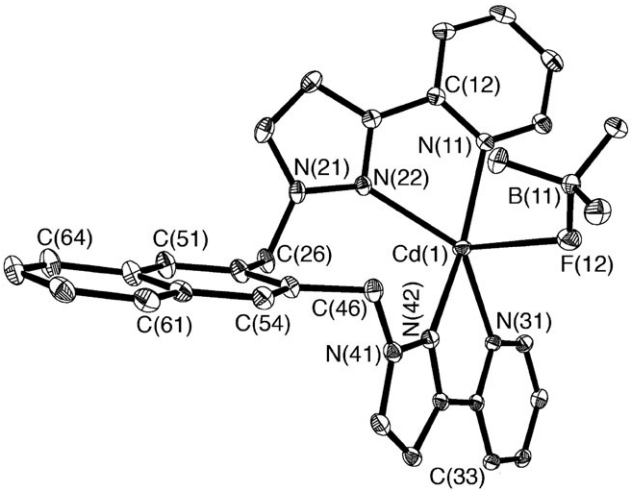

Fig. 4 Molecular structure of $[Cd(L^{naph})(BF_4)](BF_4)\cdot 2MeNO_2$ showing 40% displacement ellipsoids.

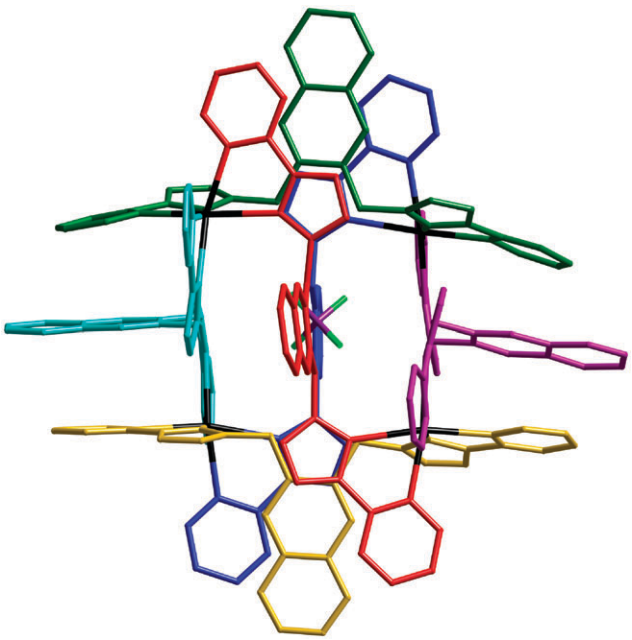

Fig. 5 A view of $[Cd_4(L^{naph})_6(BF_4)](BF_4)_7$ showing the complete cage (plus encapsulated anion) with each ligand coloured separately.

the centre of that face. Thus every F atom has three short F···H contacts with distances in the range 2.3–2.5 Å, with corresponding F···C distances in the range 3–3.2 Å, indicative of CH···F hydrogen bonds.[14] The intertwining of ligands results in π-stacked arrays in which every (π-electron-rich) naphthyl unit is sandwiched between two (π-electron-deficient) coordinated pyrazolyl–pyridine units. Slightly surprisingly the larger ionic radius of the second-row metal cation [Cd(II) *vs.* Co(II)/Zn(II)] has no effect on the overall size of the cage. Whilst the Cd–N distances are of course slightly longer than those with Co(II) or Zn(II)—in the range 2.29 to 2.41 Å, rather than the range 2.1–2.2 Å for the first row complexes[5b,f,g]—the Cd···Cd distances lie in the range 9.04–9.81 Å, a slightly *shorter* range than was observed in the Co(II) and Zn(II) cages (9.3–10 Å), implying that the bridging ligands are more folded in the Cd(II) complex. In fact the average Cd···Cd separation is 9.28 Å, compared to an average Zn···Zn separation of 9.72 Å in $[Zn_4(L^{naph})_6(BF_4)](BF_4)_7$.[5g]

The ^{1}H NMR spectrum—containing two sets of signals in an approximately 8 : 1 ratio—is therefore consistent with a *ca.* 1.33 : 1 molar mixture of cage to mononuclear complex products, since the cage contains six equivalent ligands, but the mononuclear complex only contains one ligand. A similar conclusion is obtained from the ^{19}F NMR spectrum, which contains two ^{19}F signals at −151 (major signal) and −142 ppm (minor signal), corresponding to free and trapped $[BF_4]^-$ anions, as with other cages. However in this case the ratio of the two signals was *ca.* 9 : 1 rather than the ideal 7 : 1, consistent with this mixture of species. A 1.33 : 1 mix of cage (seven free and one trapped anions) and mononuclear complex (two free anions) should give overall an 8.5 : 1 ratio of free to trapped anions, as observed by ^{19}F NMR spectroscopy.

To see if ions other than perchlorate or tetrafluoroborate could act as guests in these cages, we attempted the reaction of L^{naph} with $Zn(SiF_6)$ in a 3 : 2 ratio under ambient conditions in MeOH–$CHCl_3$. On recrystallisation of the product from nitromethane–ether a batch of small crystals was isolated of what proved to be the cage complex $[Zn_4(L^{naph})_6(SiF_6)](SiF_6)_3$, with one hexafluorosilicate anion in the central cavity of the cage and the other three outside (Fig. 6). These crystals scattered very weakly and required synchrotron radiation to get a structural determination with the conventional *R* factor being 0.158. However, the general structure of the tetrahedral cage complex is clearly defined and is exactly similar to what we have seen with all other cages of L^{naph}, so this requires no further comment.

The complex has three-fold symmetry, with the rotation axis passing through Zn(2) and the central anion [containing Si(11)], such that one third of the complex lies in the asymmetric unit, with Zn(1) and Si(21) being in general positions. The Zn···Zn separations along the edges of the cage are either 9.69 or 9.76 Å, averaging 9.73 Å, very similar to the Zn···Zn separation in $[Zn_4(L^{naph})_6(BF_4)](BF_4)_7$ despite the larger size of the guest anion which might be expected to result in expansion of the cage.[15] The F atoms of the central $[SiF_6]^{2-}$ anion are disordered so it is not appropriate to analyse the interactions of the anion with the internal surface of the cage in detail, but it is clear that there must be numerous CH···F hydrogen bonds between the anion and the methylene protons of the ligands which are directed towards the central cavity. Clearly, the larger size of $[SiF_6]^{2-}$ compared to $[BF_4]^-$—both in terms of the higher number of F atoms to be accommodated and the greater length of Si–F bonds compared to B–F bonds—does not prevent it from being accommodated in the central cavity of one of these cages.

Solution characterisation of the cage was hindered by its poor solubility. Unlike all of the cages based on uninegative counter-ions, we could not observe a molecular ion by ESMS: only small fragments at low *m*/*z* values. Also the ^{1}H NMR spectrum was uninformative, showing only broad peaks in the aromatic region. However the ^{19}F NMR spectrum in CD_3NO_2 clearly showed two peaks in an exact 3 : 1 ratio at −128 and −139 ppm, respectively [Fig. 6(b)], corresponding to three

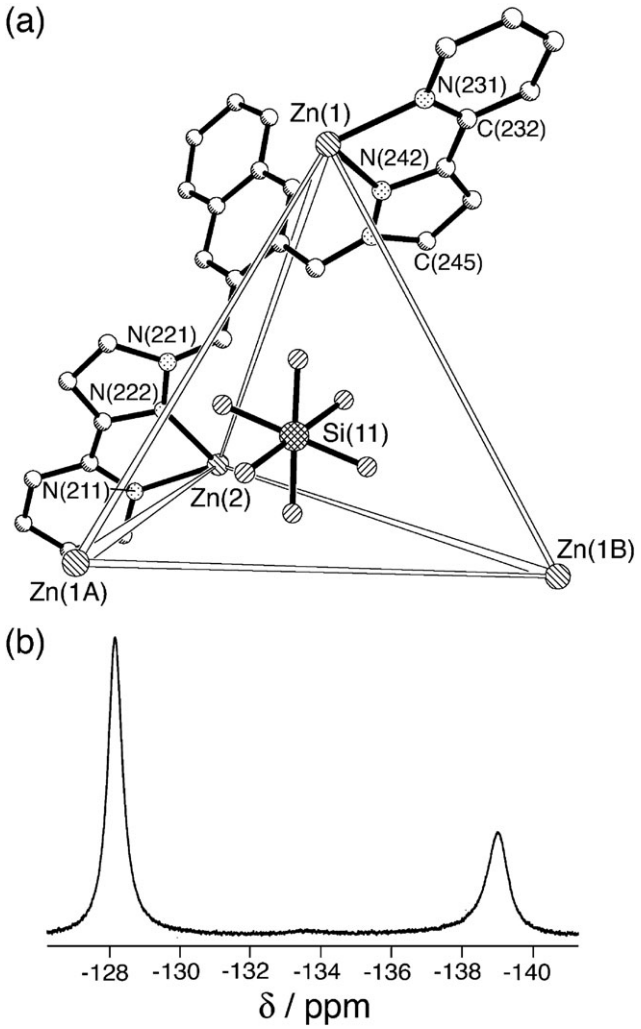

Fig. 6 (a) A view of the complex cation of $[Zn_4(L^{naph})_6(SiF_6)](SiF_6)_3$ showing the tetrahedral arrangement of Zn(II) ions, one bridging ligand, and the encapsulated anion (one of the two disordered components). (b) ^{19}F NMR spectrum (at 376.5 MHz) of $[Zn_4(L^{naph})_6(SiF_6)](SiF_6)_3$ in CD_3NO_2, showing the two signals for the free and encapsulated anions in a 3 : 1 ratio.

external and one internal anions, consistent with the cage structure being retained in solution such that exchange between internal and external anions is slow on the NMR timescale.

(iii) Preparation of $[Co_4(L^{anth})_6(BF_4)](BF_4)_7$ and assignment of ^1H NMR spectra of the Co(II) cages

Having prepared the ligand L^{anth} [part (i)] we used it to make the new cage complex $[Co_4(L^{anth})_6(BF_4)](BF_4)_7$, using the same solvothermal method that we used for the Zn(II) analogue [part (i), above]. The identity of the complex was confirmed by ES mass spectroscopy which gave a series of peaks corresponding to the cage $\{Co_4(L^{anth})_6(BF_4)_{8-n}\}^{n+}$ associated with varying numbers of anions. X-Ray crystallographic analysis was complicated by the same problem of extensive disorder that afflicted the Zn(II) complex, which led to very weak scattering, even using a rotating anode X-ray source (conventional R factor of 0.20). However it was clear that $[Co_4(L^{anth})_6(BF_4)](BF_4)_7$ is crystallographically isostructural and isomorphous with $[Zn_4(L^{anth})_6(BF_4)](BF_4)_7$, and we could confirm that the connectivity in the complex cation is as expected (*cf.* Fig. 2). ^{19}F NMR spectroscopy showed the expected two signals in an approximately 7 : 1 ratio for the external and internal tetrafluoroborate anions that are not undergoing exchange, at −144 ppm (7F, free anions) and −248 ppm (1F, encapsulated anion). In this case, the very large shift of the signal for the encapsulated anion compared to that observed in the Zn(II) complex (−140 ppm) is ascribable to the paramagnetism of the Co(II) cage.

Although the three cages $[Co_4L_6(BF_4)](BF_4)_7$ (L = L^{Ph}, L^{naph} and L^{anth}) are paramagnetic, high-spin Co(II) complexes can nevertheless lend themselves to ready analysis by ^1H NMR spectroscopy.[12,16] The ^1H NMR spectra (Fig. 7) of all three cages show a series of clearly-defined peaks between −110 and +90 ppm, with the number of signals consistent with high symmetry in solution such that all ligands are equivalent and all have two-fold symmetry, *i.e.* one half of one ligand is in a magnetically unique environment with the others being symmetry related, as observed in related cages with this series of ligands.[5f]§ Many of the signals are almost superimposable between the complexes and correspond to the four pyridyl, two pyrazolyl and two (disatereotopic) CH_2 protons which are common to all three complexes.

It is quite clear that some of the signals are much broader (and of correspondingly lower intensity) than others, because they have shorter T_1 relaxation times. Peak width is inversely proportional to T_1 for each proton, and T_1 in turn is related to the distance of the relevant proton from the paramagnetic Co(II) centres. In fact T_1^{-1} for a given proton is proportional to $\Sigma(r_{ij}^{-6})$, where r_{ij} are the pairwise distances between a particular hydrogen atom and each of the four Co(II) ions, and this relationship provides a mechanism for assigning the ^1H NMR spectra of the complexes, by correlating T_1 values for the separate peaks with $[\Sigma(r_{ij}^{-6})]^{-1}$ values for H···Co separations.[16c]

The assignments for $[Co_4(L^{naph})_6(BF_4)](BF_4)_7$ made on this basis are given in Table 2 (and are labelled in Fig. 7), which lists the $[\Sigma(r_{ij}^{-6})]^{-1}$ values for each of the independent proton environments, normalised such that the constant of proportionality is unity and the value of the smallest $[\Sigma(r_{ij}^{-6})]^{-1}$ is exactly numerically equal to the smallest T_1 values. The agreement between the normalised $[\Sigma(r_{ij}^{-6})]^{-1}$ values (based on crystallographic data) and the measured T_1 values is excellent and completely confirms the assignments. The two broadest NMR signals at +79 and −107 ppm, which have the shortest T_1 values (1.3 and 1.4 ms, respectively) correspond to pyridine H^6 and one of the CH_2 protons, respectively, which have shortest distances to Co(II) ions of 3.21 and 3.30 Å, respectively. The difference in magnetic environments of the two diastereotopic CH_2 protons is manifested in a large difference in their chemical shifts (−65 and −107 ppm).

§ The H NMR spectra of $[Co_4L_6(BF_4)](BF_4)_7$ (L = L^{Ph}, L^{naph}) were mentioned in ref. 5*f*. However they were incomplete as the two peaks at high negative chemical shift were not located at that time, and no assignment of the spectra was attempted.

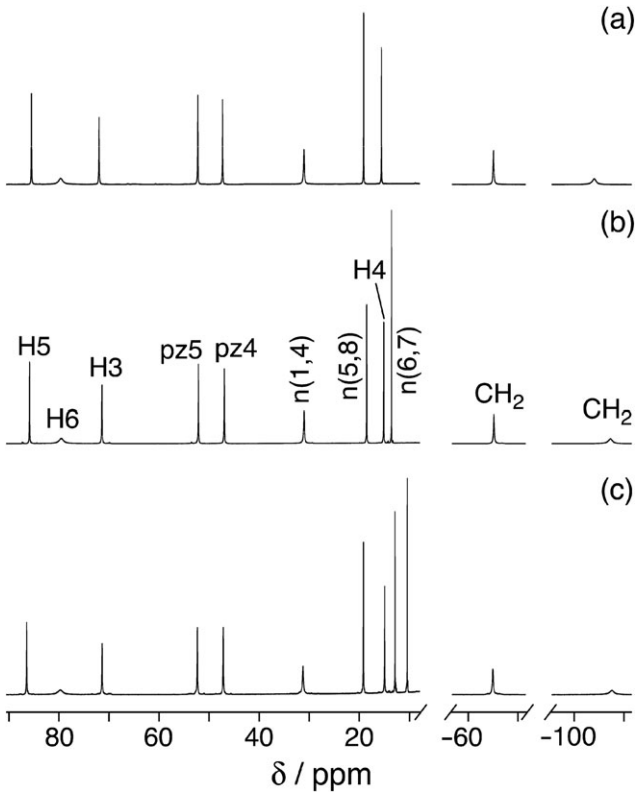

Fig. 7 400 MHz ^{1}H NMR spectra of the paramagnetic complexes (a) $[Co_4(L^{Ph})_6(BF_4)](BF_4)_7$, (b) $[Co_4(L^{naph})_6(BF_4)](BF_4)_7$, and (c) $[Co_4(L^{anth})_6(BF_4)](BF_4)_7$ in CD_3CN. Labelling on spectrum (b), determined on the basis of relaxation time measurements (see main text), follows the scheme used for Fig. 3, with *n*(1,4) denoting protons H^1 and H^4 of the naphthyl group *etc*.

(iv) Diffusion NMR measurements on the Co(II) cages

Diffusion-ordered (DOSY) NMR spectroscopy has become a valuable tool for investigating large molecules in solution,[17] and we have performed both ^{1}H and ^{19}F DOSY measurements on the cages $[Co_4L_6(BF_4)](BF_4)_7$ (L = L^{ph}, L^{naph} and L^{anth}).

^{1}H DOSY measurements were used to compare the diffusion coefficients for the free ligands L and the corresponding cage complex in every case. The solvent used was a 1 : 1 mixture of CD_3CN and $CDCl_3$, in which both free ligands and cage complexes were soluble. For free L^{ph}, L^{naph} and L^{anth}, measurements using two independent proton signals in each case (pyridyl H^6 at *ca.* 8.6 ppm and the CH_2 singlet at *ca.* 5.6 ppm) gave diffusion coefficients *D* of $1.1(1) \times 10^{-9}$, $1.0(1) \times 10^{-9}$ and $0.9(1) \times 10^{-10}$ m^2 s^{-1}, respectively, with the values of *D* decreasing slightly as the ligands increase in size. The diffusion coefficients of the corresponding cage complexes $[Co_4L_6(BF_4)](BF_4)_7$ were likewise measured using two independent ^{1}H NMR resonances and all gave very similar *D* values of $4.6(2) \times 10^{-10}$, $5.0(2) \times 10^{-10}$ and $4.4(2) \times 10^{-10}$ m^2 s^{-1}, respectively. The uncertainty on these values is larger than for the free ligands (possibly, a function of the paramagnetism) and the three *D* values are broadly comparable: most importantly, however, they are about half the values obtained for the free ligands, consistent with the fact that the cage complexes remain intact in solution and diffuse more slowly because of their greater size. In fact a halving of *D* implies a doubling of the radius (eqn (1)), and hence (for spherical particles of the same density) an increase of a factor of 8 in the molecular weight, which is approximately true when one compares the free ligands and the complex cations: for example L^{ph} has a M_W of 392, whereas $[Co_4(L^{ph})_6(BF_4)]^{7+}$ has a M_W of 2675.

Table 2 ^{1}H NMR assignment for $[Co_4(L^{naph})_6(BF_4)](BF_4)_7$ in MeCN

δ/ppm	Measured T_1/ms	Normalised $[5(r_{ij}^{-6})]^{-1}$[a]	Assignment
79.6	1.3	1.3	Pyridyl H^6
–107.3	1.4	1.5	CH_2
–65.1	7.2	6.7	CH_2
31.0	7.6	8.6	Naphthyl H^1/H^4
71.4	17.9	18.3	Pyridyl H^3
47.0	19.9	18.4	Pyrazolyl H^4
52.1	21.1	19.7	Pyrazolyl H^5
85.9	21.9	22.7	Pyridyl H^5
15.1	43.6	46.6	Pyridyl H^4
18.5	53.0	67.2	Naphthyl H^5/H^8
13.6	176	270	Naphthyl H^6/H^7

[a] Calculated from crystallographic data (ref. 5*f*) on the basis of the four different H···Co separations for each type of proton in nm (hence, in units of nm^6) and then normalised against the signal at 79.6 ppm such that this value was numerically identical to the observed relaxation time of 1.3 ms. Ideally the numbers in columns 2 and 3 should be identical; the discrepancies arise because of the uncertainties in crystallographic measurements of bond distances and also the uncertainty in T_1 measurements. Given that the measured T_1 values span a factor of *ca.* 140, the maximum discrepancy of a factor of 1.5 is very good.

$$D = k_B T/6\pi\eta r \quad (1)$$

The Stokes–Einstein equation (eqn (1)) can be used to estimate the effective radius *r* of the complex cations from their *D* values, assuming that they are approximately spherical. In eqn (1), k_B is the Boltzmann constant, *T* the temperature, η the solvent viscosity, and *r* the particle radius. At 298 K, and taking the solvent viscosity to be 0.44×10^{-3} kg m^{-1} s^{-1} (mean of the values for MeCN and chloroform), and taking *D* to be 5.0×10^{-10} (for the cage with L^{naph}), we arrive at r = 9.8 Å; taking the value of *D* to be 4.4×10^{-10} m^2 s^{-1} (for the cage with L^{anth}), we arrive at r = 11.2 Å. For these two complexes the distances from the central boron atom to the most remote peripheral proton are 10.8 and 13.2 Å, respectively, from X-ray crystallographic data.[5b,f] Given that the cages are tetrahedral and not spherical, these maximum centre-to-edge distances will be somewhat larger than the 'average' radius, and in fact we see that the calculated values of *r* from the Stokes–Einstein equation are 10–20% less than the maximal centre-to-periphery distances determined crystallographically. Accordingly the agreement between crystallographic data and NMR DOSY measurements is good.

We were next interested to see if the encapsulated tetrafluoroborate anions have similar diffusion coefficients to the surrounding cages, which would imply that the anion is tightly held in the cage cavity and not free to escape. The observation of separate ^{19}F resonances for the free and trapped anions implies that there is no exchange between them on the NMR timescale. The observation of CH···F hydrogen bonds between the central anion and ligands in the cage superstructure

suggests that the trapped anion will be locked in place and should not be able to move independently of the cage, but DOSY measurements are useful to confirm this one way or the other.

A DOSY measurement on the ^{19}F signal for NH_4BF_4 in the same solvent mixture (1 : 1 CD_3CN–$CDCl_3$) gave a D value of 2.5×10^{-9} m^2 s^{-1}. Looking next at the ^{19}F signals for the 'free' tetrafluoroborate anions in the complexes, we found in every case substantially lower D values in the range 7–8 $\times$ 10^{-10} m^2 s^{-1}. This implies that the diffusion of the seven free tetrafluoroborate anions associated with each complex cation is actually substantially retarded by ion-pairing with the complex cation that has a charge of +7. We have seen this effect elsewhere in the addition of chiral 'trisphat' anions to a solution of the racemic chiral cage $[Co_4(L^{Ph})_6(BF_4)](BF_4)_7$, which resulted in the ^{19}F signal for the trapped central anion splitting into two components for the two diastereoisomeric ion-pairs.[18]

DOSY measurements using the ^{19}F signal for the trapped tetrafluoroborate anion for each of the three cages gave D values in the range 3.7–4.1 $\times$ 10^{-10} m^2 s^{-1}, reduced by a factor of two compared to the 'free' anions in these complexes, and—crucially—similar to the values of 4.4–5.0 $\times$ 10^{-10} m^2 s^{-1} obtained for the cage superstructures using ^1H DOSY measurements. This is a reasonable agreement, within $\approx$20%, and confirms that the encapsulated anions are trapped in the central cavities with no exchange with external anions. Ideally we would see much closer agreement between the diffusion coefficients for the cage (from ^1H measurements) and the trapped anion (from ^{19}F measurements) because diffusion measurements are capable of higher accuracy than we observe. However, given the combination of (i) a comparison between two different nuclei, (ii) a mixed solvent system, and (iii) the paramagnetism of the cage, the agreement between D values for the cage and the trapped anion is acceptable, with the discrepancy being much smaller than the factor of two difference between D values for free and encapsulated anions.

Conclusions

In this paper we have reported a series of structural and spectroscopic studies on a family of isostructural M_4L_6 tetrahedral cages. The main conclusions are as follows.

(i) The new ligand L^{anth} affords, with Co(II) and Zn(II), cages of the same structural type as previously observed with L^{Ph} and L^{naph}. The fluorescence of L^{anth} is not substantially changed by incorporation of the ligand into a stacked array in the cages, in contrast to what was previously observed with L^{naph} whose fluorescence was significantly modified when incorporated into a cage.

(ii) The family of metal cations and guest anions used in these cages has been extended with two additional structurally characterised examples: one based on Cd(II), which—despite the larger size of Cd(II) compared to Co(II) and Zn(II)—affords a cage of about the same size; and one containing hexafluorosilicate as an anion, the first example of a dianion as guest in this family of cages.

(iii) The ^1H NMR spectra of the isostructural series of three Co(II) cage complexes have been fully assigned on the basis of correlating T_1 relaxation times and peak widths with X-ray crystallographic measurements of Co···H distances.

(iv) ^1H DOSY measurements have confirmed that the cage complexes are intact in solution, with diffusion coefficients commensurate with the cage sizes. ^{19}F DOSY measurements on the $[BF_4]^-$ anions show that the internal trapped anion has a diffusion coefficient about the same as the cage superstructure surrounding it—hence there is no freedom of motion of the anion inside the cavity—and also shows that the external anions have diffusion coefficients slower than 'free' $[BF_4]^-$, which can be ascribed to ion-pairing with the 7+ cation.

Experimental

Materials and methods

The following compounds were prepared using published methods: L^{naph},[5f] 3-(2-pyridyl)-pyrazole,[19] 2,3-bis(bromomethyl)-anthracene,[20] $[Co_4(L^{ph})_6(BF_4)](BF_4)_7$,[5b] and $[Co_4(L^{naph})_6(BF_4)](BF_4)_7$.[5f] All other chemicals were purchased from Aldrich and were used as received. The following instruments were used for routine spectroscopic measurements: UV/Vis spectra, a Cary 50 spectrophotometer; luminescence spectra, a Jobin-Yvon Fluoromax 4 fluorimeter; EI mass spectra, a VG AutoSpec magnetic sector instrument; ES mass spectra, a Waters LCT instrument; ^1H NMR spectra, Bruker AV1-250 or AV3-400 spectrometers. For the DOSY measurements the probe gradient power was calibrated using a standard 0.3 M $GdCl_3$ solution in D_2O containing 1% H_2O and 0.1% CH_3OH.

Synthesis of L^{anth}. 2,3-Bis(bromomethyl)anthracene (0.50 g, 1.37 mmol) and 3-(2-pyridyl)pyrazole (0.40 g, 2.70 mmol) were dissolved in THF (60 cm^3) to which aqueous NaOH (5.5 M, 5 cm^3) was added. The resulting mixture was heated to reflux for 20 h, before being allowed to cool to room temperature. The organic layer was extracted and filtered through $MgSO_4$ before being evaporated to dryness. The resultant crude orange powder was purified by column chromatography on activated alumina, eluting with DCM–MeOH (99 : 1, v/v) to give pure L^{anth} (0.36 g, 54%). Anal. calcd for $C_{32}H_{24}N_6$: C, 78.0; H, 4.9; N, 17.1%. Found: C, 77.6; H, 4.5; N, 16.8%. ESMS: m/z 493 $(M + H)^+$, 515 $(M + Na)^+$. ^1H NMR (400 MHz, $CDCl_3$): δ 8.67 (2H, ddd, J = 4.8, 1.8, 0.8 Hz, pyridyl H^6), 8.39 (2H, s; anthryl H), 8.00 (2H, dd, J = 7.8, 3.2 Hz; anthryl H) overlapping with 8.00 (2H, d, J = 8.0 Hz, pyridyl H^3), 7.78 (2H, s, anthryl H), 7.74 (2H, td, J = 7.6, 1.6 Hz, pyridyl H^4), 7.50 (2H, dd, J = 6.4, 3.2 Hz, anthryl H), 7.47 (2H, d, J = 2.4 Hz, pyrazolyl H^5), 7.23 (2H, ddd, J = 7.7, 4.8, 0.8 Hz, pyridyl H^5), 6.98 (2H, d, J = 2.4 Hz, pyrazolyl H^4), 5.61 (4H, s, CH_2).

Syntheses of complexes

The complexes $[Zn_4(L^{anth})_6(BF_4)](BF_4)_7$, $[Co_4(L^{anth})_6(BF_4)](BF_4)_7$ and $[Cd_4(L^{naph})_6(BF_4)](BF_4)_7$ were all prepared solvothermally; the method given here for $[Zn_4(L^{anth})_6(BF_4)](BF_4)_7$ is typical. A Teflon-lined autoclave was charged with $Zn(BF_4)\cdot xH_2O$ (0.016 g, 0.07 mmol), L^{anth} (0.05 g, 0.1 mmol) and methanol (9 cm^3). Heating to 100 °C for 12 h followed by slow cooling to room temperature yielded yellow prismatic crystals directly from the cooled reaction mixture. All crystalline samples for elemental analysis were dried thoroughly *in vacuo* and proved to be hygroscopic, gaining weight when exposed to air; consequently all C, H,

N, analytical data are consistent with the presence of several water molecules per complex molecule.

Data for $[Zn_4(L^{anth})_6(BF_4)](BF_4)_7$: yield 68%. ESMS: m/z 278, $\{Zn(L^{anth})\}^{2+}$. NMR: see main text. Anal. found: C, 56.7; H, 3.9; N, 12.3%. Required for $[Zn_4(L^{anth})_6(BF_4)](BF_4)_7{\cdot}9H_2O$: C, 56.6; H, 4.0; N, 12.4%.

Data for $[Co_4(L^{anth})_6(BF_4)](BF_4)_7$: yield 73%. ESMS: m/z 1208, $\{[Co_4(L^{anth})_6][BF_4]_5\}^{3+}$; 885, $\{[Co_4(L^{anth})_6][BF_4]_4\}^{4+}$; 690 $\{[Co_4(L^{anth})_6][BF_4]_3\}^{5+}$. NMR: see main text. Anal. found: C, 57.2; H, 4.3; N, 11.9%. Required for $[Co_4(L^{anth})_6(BF_4)](BF_4)_7{\cdot}9H_2O$: C, 57.0; H, 4.0; N, 12.5%.

Data for $[Cd_4(L^{naph})_6(BF_4)](BF_4)_7$. This was isolated as a mixture containing also mononuclear $[Cd(L^{naph})(BF_4)](BF_4)$ (see main text). ESMS of the mixture: m/z 1085, $\{Cd(L^{naph})_2(BF_4)\}^{+}$; 720, $\{Cd(L^{naph})_3\}^{2+}$; 683, $\{Cd(L^{naph})(BF_4)\}^{+}$; 499, $\{Cd(L^{naph})_2\}^{2+}$.

$[Zn_4(L^{naph})_6(SiF_6)](SiF_6)_3$ was prepared under ambient conditions as follows. Solutions of $Zn(SiF_6){\cdot}xH_2O$ (0.016 g, 0.075 mmol) in MeOH (7.5 cm^3) and L^{naph} (0.050 g, 0.1 mmol) in chloroform (7.5 cm^3) were combined and the resulting solution was vigorously stirred for 24 h. The solvent was subsequently removed under vacuum and the crude powder was washed with methanol and then chloroform to remove any unreacted starting materials. Diethyl ether was allowed to slowly diffuse into a solution of the dried white powder in nitromethane. X-Ray quality prismatic crystals grew on standing within one week (0.023 g, 43%). Anal. found: C, 52.6; H, 3.9; N, 13.0%. Required for $[Zn_4(L^{naph})_6(SiF_6)](SiF_6)_3{\cdot}19H_2O$: C, 52.7; H, 4.4; N, 13.2%.

X-Ray crystallography‡

Data for L^{anth}, $[Cd_4(L^{naph})_6(BF_4)](BF_4)_7{\cdot}5MeOH{\cdot}3H_2O$ and $[Cd(L^{naph})(BF_4)](BF_4){\cdot}2MeNO_2$ were collected at the University of Sheffield on a Bruker APEX 2 diffractometer using graphite-monochromated Mo-Kα X-radiation (0.71073 Å). Data for $[Zn_4(L^{anth})_6(BF_4)](BF_4)_7$ were collected at the University of Leeds on a Bruker APEX 2 diffractometer using graphite-monochromated Mo-Kα X-radiation (0.71073 Å) from a rotating anode source. Data for $[Zn_4(L^{naph})_6(SiF_6)](SiF_6)_3$ were collected at the Daresbury Synchrotron Radiation Source (station 9.8) on a Bruker APEX 2 diffractometer using Si(111)-monochromated synchrotron radiation with a wavelength (λ = 0.6926 Å) close to the Zr absorption edge. As mentioned in the main text, crystals of the cage complexes scattered weakly due to the extensive disorder of anions and solvent molecules and {for $[Zn_4(L^{anth})_6(BF_4)](BF_4)_7$} of the entire cage. After integration of the raw data, and before merging, an empirical absorption correction was applied (SADABS)[21] based on comparison of multiple symmetry-equivalent measurements. The structures were solved by direct methods and refined by full-matrix least squares on weighted F^2 values for all reflections using the SHELX suite of programs.[22] Crystallographic data are collected in Table 1.

The structural determinations of L^{anth} and $[Cd(L^{naph})(BF_4)](BF_4){\cdot}2MeNO_2$ were straightforward and presented no problems. For $[Cd_4(L^{naph})_6(BF_4)](BF_4)_7{\cdot}5MeOH{\cdot}3H_2O$, only six of the eight $[BF_4]^-$ anions could be clearly located with the other two being subsumed into a diffuse area of electron density that could not be satisfactorily modelled and which no doubt also included disordered solvent molecules. The SQUEEZE function in PLATON[23] was used to eliminate these areas of electron density form the refinement; more details of this, and the disorder of those anions and solvent molecules that were located, are in the CIF‡.

The structural determination of $[Zn_4(L^{anth})_6(BF_4)](BF_4)_7$ was particularly difficult because of the superposition of both enantiomers, as mentioned in the main text. This required all pyridyl and pyrazole rings, and metal ions, to be modelled over two sites with extensive use of geometric restraints to keep the ligand geometries reasonable. Only four of the eight $[BF_4]^-$ anions could be clearly located and likewise required heavy geometric restraints to keep the refinement stable. The SQUEEZE function in PLATON[22] was used to eliminate large areas of diffuse electron density which, presumably, contained a disordered mixture of the remaining anions and solvent molecules. Full details are in the CIF‡.

For $[Zn_4(L^{naph})_6(SiF_6)](SiF_6)_3$ the data were very weak even using synchrotron radiation and extensive use of geometric restraints was required for the aromatic rings of the ligands, and the counter-ions. Both anions displayed disorder of their F atoms. The F atoms attached to Si(11) (inside the cage cavity) were all disordered over two sites. For Si(21), a *trans* axial pair of F atoms are ordered, with the other four in the 'equatorial' plane all disordered over two sites. Areas of electron density close to special positions suggested the presence of solvent molecules which however could not be modelled satisfactorily; these were removed from the refinement using the SQUEEZE function in PLATON;[22] full details are in the CIF‡.

Acknowledgements

We thank the EPSRC (UK) for a post-doctoral research fellowship (to I. T.), and for funding of the UK National Crystallography Service. We also thank STFC (UK) for access to synchrotron facilities.

References

1 Reviews on coordination cages: (*a*) G. F. Swiegers and T. J. Malefetse, *Coord. Chem. Rev.*, 2002, **225**, 91; (*b*) M. Fujita, M. Tominaga, A. Hori and B. Therrien, *Acc. Chem. Res.*, 2005, **38**, 369; (*c*) D. Fiedler, D. H. Leung, R. G. Bergman and K. N. Raymond, *Acc. Chem. Res.*, 2005, **38**, 349; (*d*) T. D. Hamilton and L. R. MacGillivray, *Cryst. Growth Des.*, 2004, **4**, 419; (*e*) M. D. Ward, in *Organic Nanostructures*, ed. J. Atwood, J. Steed, Wiley, Weinheim, 2008; (*f*) A. L. Garay, A. Pichon and S. L. James, *Chem. Soc. Rev.*, 2007, **36**, 846; (*g*) S. Alvarez, *Dalton Trans.*, 2006, 2209; (*h*) R. W. Saalfrank, E. Uller, B. Demleitner and I. Bernt, *Struct. Bonding*, 2000, **96**, 149; (*i*) P. J. Stang and S. R. Seidel, *Acc. Chem. Res.*, 2002, **35**, 972; (*j*) R. W. Saalfrank and B. Demleitner, in *Perspectives in Supramolecular Chemistry*, ed. J.-P. Sauvage, John Wiley & Sons Ltd., Chichester, UK, 1999, vol. 5, pp. 1–51.
2 (*a*) X. K. Sun, D. W. Johnson, D. L. Caulder, K. N. Raymond and E. H. Wong, *J. Am. Chem. Soc.*, 2001, **123**, 2752; (*b*) M. Fujita, K. Umemoto, M. Yoshizawa, N. Fujita, T. Kusukawa and K. Biradha, *Chem. Commun.*, 2001, 509; (*c*) D. A. Caulder and K. N. Raymond, *J. Chem. Soc., Dalton Trans.*, 1999, 1185.
3 (*a*) A. V. Davis, D. Fiedler, G. Seeber, A. Zahl, R. van Eldik and K. N. Raymond, *J. Am. Chem. Soc.*, 2006, **128**, 1324; (*b*) D. W. Johnson and K. N. Raymond, *Inorg. Chem.*, 2001, **40**,

5157; (*c*) T. Brassey, R. Scopelliti and K. Severin, *Chem. Commun.*, 2006, 3308; (*d*) S. Hiraoka, Y. Kubota and M. Fujita, *Chem. Commun.*, 2000, **16**, 1509.
4 (*a*) T. Yamaguchi and M. Fujita, *Angew. Chem., Int. Ed.*, 2008, **47**, 2067; (*b*) Y. Nishioka, T. Yamaguchi, M. Yoshizawa and M. Fujita, *J. Am. Chem. Soc.*, 2007, **129**, 7000; (*c*) K. Takaoka, M. Kawano, T. Ozeki and M. Fujita, *Chem. Commun.*, 2006, 1625; (*d*) M. Yoshizawa and M. Fujita, *Pure Appl. Chem.*, 2005, **77**, 1107; (*e*) T. S. Koblenz, J. Wassenaar and J. N. H. Reek, *Chem. Soc. Rev.*, 2008, **37**, 247; (*f*) A. W. Kleij and J. N. H. Reek, *Chem.–Eur. J.*, 2006, **12**, 4219; (*g*) D. H. Leung, R. G. Bergman and K. N. Raymond, *J. Am. Chem. Soc.*, 2006, **128**, 9781.
5 (*a*) R. W. Saalfrank, R. Burak, A. Breit, D. Stalke, R. Herbst-Irmer, J. Daub, M. Porsch, E. Bill, M. Muther and A. X. Trautwein, *Angew. Chem., Int. Ed. Engl.*, 1994, **33**, 1621; (*b*) J. S. Fleming, K. L. V. Mann, C.-A. Carraz, E. Psillakis, J. C. Jeffery, J. A. McCleverty and M. D. Ward, *Angew. Chem., Int. Ed.*, 1998, **37**, 1279; (*c*) R. L. Paul, S. P. Argent, J. C. Jeffery, L. P. Harding, J. M. Lynam and M. D. Ward, *Dalton Trans.*, 2004, 3453; (*d*) J. K. Clegg, L. F. Lindoy, B. Moubaraki, K. S. Murray and J. C. McMurtrie, *Dalton Trans.*, 2004, 2417; (*e*) A. V. Davis, D. Fiedler, M. Ziegler, A. Terpin and K. N. Raymond, *J. Am. Chem. Soc.*, 2007, **129**, 15354; (*f*) R. L. Paul, Z. R. Bell, J. C. Jeffery, J. A. McCleverty and M. D. Ward, *Proc. Natl. Acad. Sci. U. S. A.*, 2002, **99**, 4883; (*g*) R. L. Paul, Z. R. Bell, J. C. Jeffery, L. P. Harding, J. A. McCleverty and M. D. Ward, *Polyhedron*, 2003, **22**, 781.
6 (*a*) A. J. Amoroso, J. C. Jeffery, P. L. Jones, J. A. McCleverty, P. Thornton and M. D. Ward, *Angew. Chem., Int. Ed. Engl.*, 1995, **34**, 1443; (*b*) M. Albrecht, I. Janser, S. Burk and P. Weis, *Dalton Trans.*, 2006, 2875; (*c*) R. M. Yeh, J. Xu, G. Seeber and K. N. Raymond, *Inorg. Chem.*, 2005, **44**, 6228.
7 (*a*) Z. R. Bell, L. P. Harding and M. D. Ward, *Chem. Commun.*, 2003, 2432; (*b*) S. P. Argent, H. Adams, L. P. Harding and M. D. Ward, *Dalton Trans.*, 2006, 542.
8 (*a*) Z. R. Bell, J. C. Jeffery, J. A. McCleverty and M. D. Ward, *Angew. Chem., Int. Ed.*, 2002, **41**, 2515; (*b*) S. P. Argent, H. Adams, T. Riis-Johannessen, J. C. Jeffery, L. P. Harding, O. Mamula and M. D. Ward, *Inorg. Chem.*, 2006, **45**, 3905.
9 (*a*) S. P. Argent, H. Adams, T. Riis-Johannessen, J. C. Jeffery, L. P. Harding and M. D. Ward, *J. Am. Chem. Soc.*, 2006, **128**, 72; (*b*) N. K. Al-Rasbi, I. Tidmarsh, S. P. Argent, H. Adams, L. P. Harding and M. D. Ward, *J. Am. Chem. Soc.*, 2008, **130**, 11641.
10 (*a*) R. W. Saalfrank, A. Stark, K. Peters and H. G. von Schnering, *Angew. Chem., Int. Ed. Engl.*, 1988, **27**, 851; (*b*) R. W. Saalfrank, A. Stark, M. Bremer and H.-U. Hummel, *Angew. Chem., Int. Ed. Engl.*, 1990, **29**, 311.
11 N. K. Al-Rasbi, C. Sabatini, F. Barigelletti and M. D. Ward, *Dalton Trans.*, 2006, 4769.
12 I. Tidmarsh, T. B. Faust, H. Adams, L. P. Harding, L. Russo, W. Clegg and M. D. Ward, *J. Am. Chem. Soc.*, 2008, **130**, 15167.
13 A. W. Addison, T. N. Rao, J. Reedijk, J. van Rijn and G. C. Verschoor, *J. Chem. Soc., Dalton Trans.*, 1984, 1349.
14 (*a*) F. Grepioni, G. Cojazzi, S. M. Draper, N. Scully and D. Braga, *Organometallics*, 2998, **17**, 296; (*b*) G. Desiraju and T. Steiner, *The Weak Hydrogen Bond in Structural Chemistry and Biology*, Oxford University Press, Oxford, 1999.
15 S. Mecozzi and J. Rebek, Jr, *Chem.–Eur. J.*, 1998, **4**, 1016.
16 (*a*) E. C. Constable, R. Martínez-Máñez, A. M. W. Cargill Thompson and J. V. Walker, *J. Chem. Soc., Dalton Trans.*, 1994, 1585; (*b*) E. C. Constable, M. A. M. Daniels, M. G. B. Drew, D. A. Tocher, J. V. Walker and P. D. Wood, *J. Chem. Soc., Dalton Trans.*, 1993, 1947; (*c*) H. Amouri, L. Mimassi, M. N. Rager, B. E. Mann, C. Guyard-Duhayon and L. Raehm, *Angew. Chem., Int. Ed.*, 2005, **44**, 4543.
17 (*a*) C. J. Sumby, J. Fisher, T. J. Prior and M. J. Hardie, *Chem.–Eur. J.*, 2006, **12**, 2945; (*b*) V. V. Krishnan, *J. Magn. Reson.*, 1997, **124**, 468; (*c*) T. Haino, M. Kobayashi, M. Chikaraishi and Y. Fukazawa, *Chem. Commun.*, 2005, 2321; (*d*) F. W. Kotch, V. Sidorov, Y.-F. Lam, K. J. Kayser, H. Li, M. S. Kaucher and J. T. Davis, *J. Am. Chem. Soc.*, 2003, **125**, 15140; (*e*) A. Westcott, J. Fisher, L. P. Harding, P. Rizkallah and M. J. Hardie, *J. Am. Chem. Soc.*, 2008, **130**, 2950.
18 R. Frantz, C. S. Grange, N. K. Al-Rasbi, M. D. Ward and J. Lacour, *Chem. Commun.*, 2007, 1459.
19 A. J. Amoroso, A. M. C. Thompson, J. C. Jeffery, P. L. Jones, J. A. McCleverty and M. D. Ward, *J. Chem. Soc., Chem. Commun.*, 1994, 2751.
20 J.-F. Lohier, K. Wright, C. Peggion, F. Formaggio, C. Toniolo, M. Wakselman and J.-P. Mazaleyrat, *Tetrahedron*, 2006, **62**, 6203 and references therein.
21 G. M. Sheldrick, *SADABS: a program for absorption correction with the Siemens SMART system*, University of Göttingen, Germany, 1996.
22 G. M. Sheldrick, *Acta Crystallogr., Sect. A: Found. Crystallogr.*, 2008, **64**, 112.
23 A. L. Spek, *J. Appl. Crystallogr.*, 2003, **36**, 7.